

The Possible $J^{PC} = 0^{--}$ Charmonium-like State

Wei Chen*

*Department of Physics and State Key Laboratory of Nuclear Physics and Technology
Peking University, Beijing 100871, China*

Shi-Lin Zhu†

*Department of Physics and State Key Laboratory of Nuclear Physics and Technology
and Center of High Energy Physics, Peking University, Beijing 100871, China*

We study the possible charmonium-like states with $J^{PC} = 0^{--}, 0^{-+}$ using the tetraquark interpolating currents with the QCD sum rules approach. The extracted masses are around 4.5 GeV for the 0^{--} charmonium-like states and 4.6 GeV for the 0^{-+} charmonium-like states while their bottomonium-like analogues lie around 10.6 GeV. We also discuss the possible decay, production and the experiment search of the 0^{--} charmonium-like state.

PACS numbers: 12.38.Lg, 11.40.-q, 12.39.Mk

Keywords: Charmonium-like states, QCD sum rule

I. INTRODUCTION

Since Belle collaboration observed the narrow state $X(3872)$ on the threshold of $D^0\bar{D}^0^*$ in the $B^+ \rightarrow K^+ X(3872) \rightarrow K^+ J/\psi \pi^+ \pi^-$ channel in 2003 [1], many new charmonium or charmonium-like states have been observed such as $Y(3940), Y(4260), Z(3930), X(3940), Y(4325), Y(4360), Z^+(4460), Z^+(4430), Z^+(4050), Z^+(4250)$ and $Y(4140)$ [2–11]. For experimental reviews, one can consult Refs. [12–15].

The discovery of these new states have enriched the charmonium spectroscopy greatly. It's very difficult to accommodate all these states in the conventional quark model. In order to study their underlying structure, many interpretations were proposed such as the hybrid mesons, the molecular or tetraquark states, baryonium states and so on. For example, $X(3872)$ was speculated to be a hybrid charmonium state in Ref. [16], a $D^0\bar{D}^0^*$ molecular state in Ref.[17] and a $cq\bar{c}\bar{q}$ tetraquark state in Ref. [18]. $Z^+(4430)$ was assigned as a $D^*\bar{D}_1$ molecular state in Ref. [19] and a $cs\bar{s}\bar{s}$ tetraquark state in Ref. [20]. $Y(4260)$ was proposed as a hybrid charmonium state in Ref. [21] and a $cq\bar{c}\bar{q}$ tetraquark state in Ref. [22]. $Y(4140)$ was proposed as a $D_s^*\bar{D}_s^*$ molecular state in Ref. [23]. However, one should be very cautious that the conventional charmonium spectrum may be distorted if one considers either the coupled-channel effect or the screened linear confinement force [24]. More charmonium states can be accommodated below 5 GeV within this picture [24].

The possible $c\bar{c}q\bar{q}$ states with various quantum numbers including $J^{PC} = 0^{--}$ were investigated extensively in Ref. [25] in the early 1980s. The author discussed the spectroscopy, decay and production of the $c\bar{c}q\bar{q}$ systems with the angular momentum $L \geq 1$ by taking account of the color magnetic and electric forces. In the conventional quark model, states with $J^{PC} = 0^{--}$ are exotic states. They cannot be composed of a pair of quark and antiquark. In Ref. [26], we noticed that the light tetraquark currents with $J^{PC} = 0^{--}$ do not support a low-lying resonant signal below 2 GeV. Since increasing the quark mass reduces the kinetic energy and thus may help stabilize the system, we will study whether the $c\bar{c}q\bar{q}$ states with $J^{PC} = 0^{--}$ exist in this paper.

The paper is organized as follows. We construct the tetraquark currents with $J^{PC} = 0^{--}, 0^{-+}$ using the diquark and antidiquark fields in Sec. II and derive the spectral densities in Sec. III which are collected in the Appendix. We perform the numerical analysis and extract the masses in Sec. IV and discuss the possible decay, production and the experiment search of the 0^{--} charmonium-like states in the last section.

II. TETRAQUARK INTERPOLATING CURRENTS

We have constructed the light tetraquark interpolating currents with $J^{PC} = 0^{--}$ using the diquark-antidiquark fields in the previous work [26]. In this work we follow the same steps. We first construct ten color singlet pseudoscalar

*Electronic address: boy@pku.edu.cn

†Electronic address: zhsl@pku.edu.cn

operators considering both the Lorentz and color structures: $S_6, P_6, V_6, A_6, T_6, S_3, P_3, V_3, A_3, T_3$. The subscripts **6** and **3** indicate that the color structures of the tetraquark are **6** \otimes **6̄** and **3̄** \otimes **3** respectively. Details can be found in Ref.[26]. With the charge-conjugation transformation we get

$$\mathbb{C}S_6\mathbb{C}^{-1} = V_6, \mathbb{C}A_6\mathbb{C}^{-1} = P_6, \mathbb{C}A_3\mathbb{C}^{-1} = P_3, \mathbb{C}S_3\mathbb{C}^{-1} = V_3, \mathbb{C}T_6\mathbb{C}^{-1} = T_6, \mathbb{C}T_3\mathbb{C}^{-1} = T_3. \quad (1)$$

Using the above charge-conjugation relations, we can obtain the currents with definite C parity:

1. For the quantum number $J^{PC} = 0^{--}$:

$$\begin{aligned} \eta_1 &= S_6 - V_6 = q_a^T C c_b (\bar{q}_a \gamma_5 C \bar{c}_b^T + \bar{q}_b \gamma_5 C \bar{c}_a^T) - q_a^T C \gamma_5 c_b (\bar{q}_a C \bar{c}_b^T + \bar{q}_b C \bar{c}_a^T), \\ \eta_2 &= A_6 - P_6 = q_a^T C \gamma_\mu c_b (\bar{q}_a \gamma^\mu \gamma_5 C \bar{c}_b^T + \bar{q}_b \gamma^\mu \gamma_5 C \bar{c}_a^T) - q_a^T C \gamma_\mu \gamma_5 c_b (\bar{q}_a \gamma^\mu C \bar{c}_b^T + \bar{q}_b \gamma^\mu C \bar{c}_a^T), \\ \eta_3 &= A_3 - P_3 = q_a^T C \gamma_\mu c_b (\bar{q}_a \gamma^\mu \gamma_5 C \bar{c}_b^T - \bar{q}_b \gamma^\mu \gamma_5 C \bar{c}_a^T) - q_a^T C \gamma_\mu \gamma_5 c_b (\bar{q}_a \gamma^\mu C \bar{c}_b^T - \bar{q}_b \gamma^\mu C \bar{c}_a^T), \\ \eta_4 &= S_3 - V_3 = q_a^T C c_b (\bar{q}_a \gamma_5 C \bar{c}_b^T - \bar{q}_b \gamma_5 C \bar{c}_a^T) - q_a^T C \gamma_5 c_b (\bar{q}_a C \bar{c}_b^T - \bar{q}_b C \bar{c}_a^T). \end{aligned} \quad (2)$$

2. For the quantum number $J^{PC} = 0^{-+}$:

$$\begin{aligned} \eta_5 &= S_6 + V_6 = q_a^T C c_b (\bar{q}_a \gamma_5 C \bar{c}_b^T + \bar{q}_b \gamma_5 C \bar{c}_a^T) + q_a^T C \gamma_5 c_b (\bar{q}_a C \bar{c}_b^T + \bar{q}_b C \bar{c}_a^T), \\ \eta_6 &= T_3 = q_a^T C \sigma_{\mu\nu} c_b (\bar{q}_a \sigma^{\mu\nu} \gamma_5 C \bar{c}_b^T - \bar{q}_b \sigma^{\mu\nu} \gamma_5 C \bar{c}_a^T), \\ \eta_7 &= A_6 + P_6 = q_a^T C \gamma_\mu c_b (\bar{q}_a \gamma^\mu \gamma_5 C \bar{c}_b^T + \bar{q}_b \gamma^\mu \gamma_5 C \bar{c}_a^T) + q_a^T C \gamma_\mu \gamma_5 c_b (\bar{q}_a \gamma^\mu C \bar{c}_b^T + \bar{q}_b \gamma^\mu C \bar{c}_a^T), \\ \eta_8 &= A_3 + P_3 = q_a^T C \gamma_\mu c_b (\bar{q}_a \gamma^\mu \gamma_5 C \bar{c}_b^T - \bar{q}_b \gamma^\mu \gamma_5 C \bar{c}_a^T) + q_a^T C \gamma_\mu \gamma_5 c_b (\bar{q}_a \gamma^\mu C \bar{c}_b^T - \bar{q}_b \gamma^\mu C \bar{c}_a^T), \\ \eta_9 &= S_3 + V_3 = q_a^T C c_b (\bar{q}_a \gamma_5 C \bar{c}_b^T - \bar{q}_b \gamma_5 C \bar{c}_a^T) + q_a^T C \gamma_5 c_b (\bar{q}_a C \bar{c}_b^T - \bar{q}_b C \bar{c}_a^T), \\ \eta_{10} &= T_6 = q_a^T C \sigma_{\mu\nu} c_b (\bar{q}_a \sigma^{\mu\nu} \gamma_5 C \bar{c}_b^T + \bar{q}_b \sigma^{\mu\nu} \gamma_5 C \bar{c}_a^T). \end{aligned} \quad (3)$$

It is understood that Eqs. (2)-(3) should contain $(uc\bar{u}\bar{c} + dc\bar{d}\bar{c})$ in order to have definite isospin and G -parity. Due to the SU(2) flavor symmetry, we do not differentiate the *up* and *down* quarks in our analysis and denote them by q .

III. QCD SUM RULE

QCD sum rule is a powerful approach to study the hadron properties in the past several decades[29–31]. We consider the two-point correlation function:

$$\Pi(q^2) \equiv \int d^4x e^{iqx} \langle 0 | T\eta(x)\eta^\dagger(0) | 0 \rangle, \quad (4)$$

where η is an interpolating current. At the hadron level, the correlation function $\Pi(q^2)$ is expressed via the dispersion relation:

$$\Pi^{phen}(p^2) = \int_0^\infty \frac{\rho^{phen}(s)}{s - p^2 - i\epsilon}. \quad (5)$$

The spectral function reads:

$$\begin{aligned} \rho^{phen}(s) &\equiv \sum_n \delta(s - m_n^2) \langle 0 | \eta | n \rangle \langle n | \eta^\dagger | 0 \rangle \\ &= f_X^2 \delta(s - m_X^2) + \text{continuum}, \end{aligned} \quad (6)$$

where the usual pole plus continuum parametrization of the hadronic spectral density is adopted. f_X is the overlapping parameter of the current to the pseudoscalar state X : $\langle 0 | \eta | X \rangle = f_X$.

At the quark-gluon level, the spectral density can be evaluated up to dimension eight with the same method in Refs.[18, 20, 32, 33]. Omitting the light quark mass, we use the coordinate-space expression for the light quark propagator and momentum-space expression for the charm quark propagator:

$$iS_q^{ab}(x) = \frac{i\delta^{ab}}{2\pi^2 x^4} \hat{x} + \frac{i}{32\pi^2} \frac{\lambda_{ab}^n}{2} g_s G_{\mu\nu}^n \frac{1}{x^2} (\sigma^{\mu\nu} \hat{x} + \hat{x} \sigma^{\mu\nu}) - \frac{\delta^{ab}}{12} \langle \bar{q}q \rangle + \frac{\delta^{ab} x^2}{192} \langle \bar{q}g_s \sigma \cdot G q \rangle,$$

$$\begin{aligned} iS_c^{ab}(p) = & \frac{i\delta^{ab}}{\hat{p} - m_c} + \frac{i}{4}g_s \frac{\lambda_{ab}^n}{2} G_{\mu\nu}^n \frac{\sigma^{\mu\nu}(\hat{p} + m_c) + (\hat{p} + m_c)\sigma^{\mu\nu}}{(p^2 - m_c^2)^2} + \frac{i\delta^{ab}}{12} \langle g_s^2 GG \rangle m_c \frac{p^2 + m_c \hat{p}}{(p^2 - m_c^2)^4} \\ & - \frac{i\delta^{ab}}{48} \langle g_s^3 f GGG \rangle \frac{(p^2 + 7m_c^2)\hat{p} + 2m_c(3p^2 + m_c^2)}{(p^2 - m_c^2)^5} \end{aligned} \quad (7)$$

where $\hat{x} \equiv \gamma_\mu x^\mu$, $\hat{p} \equiv \gamma_\mu p^\mu$, $\langle \bar{q}g_s\sigma \cdot Gq \rangle = \langle g_s \bar{q}\sigma^{\mu\nu}G_{\mu\nu}q \rangle$, $\langle g_s^2 GG \rangle = \langle g_s^2 G_{\mu\nu}G^{\mu\nu} \rangle$, $\langle g_s^3 f GGG \rangle = \langle g_s^3 f^{abc}G_{\gamma\delta}^a G_{\delta\epsilon}^b G_{\epsilon\gamma}^c \rangle$, a and b are the color indices. The momentum-space propagator with three soft gluon lines can be found in Ref. [30]. For the light quark propagator, we use the D dimension coordinate-space expression. The dimensional regularization is used throughout our calculation. The $\Pi(q^2)$ in the OPE side can be written as:

$$\Pi^{OPE}(p^2) = \int_{4m_c^2}^{\infty} \frac{\rho^{OPE}(s)}{s - p^2 - i\epsilon}, \quad (8)$$

Performing Borel transformation for the correlation function, we arrive at:

$$f_X^2 e^{-m_X^2/M_B^2} = \int_{4m_c^2}^{s_0} ds e^{-s/M_B^2} \rho^{OPE}(s). \quad (9)$$

where s_0 is the threshold parameter. The mass M_X reads:

$$m_X^2 = \frac{\int_{4m_c^2}^{s_0} ds e^{-s/M_B^2} s \rho^{OPE}(s)}{\int_{4m_c^2}^{s_0} ds e^{-s/M_B^2} \rho^{OPE}(s)}. \quad (10)$$

For all the tetraquark currents in Eqs. (2) and (3), we collect the $\rho^{OPE}(s)$ in the Appendix. Both the quark condensate $\langle \bar{q}q \rangle$ and quark gluon mixed condensate $\langle \bar{q}g_s\sigma \cdot Gq \rangle$ vanish in the chiral limit $m_q = 0$. One may wonder whether the quark condensates proportional to the charm quark mass: $m_c \langle \bar{q}q \rangle$ and $m_c \langle \bar{q}g_s\sigma \cdot Gq \rangle$ exist. They are usually very important corrections in the scalar, vector and axial-vector channels [18, 33, 36, 37]. However, these terms also vanish in the pseudoscalar channel. The diagrams in the same row in Fig.1 cancel out exactly due to the special Lorenz structures of the currents.

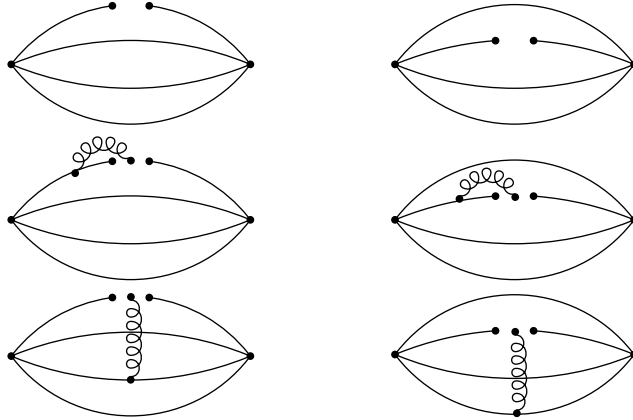


FIG. 1: Feynman diagrams for $m_c \langle \bar{q}q \rangle$ and $m_c \langle \bar{q}g_s\sigma \cdot Gq \rangle$. The diagrams in the same row cancel out exactly. In each diagram, the two upper lines represent the light quark propagators and the two lower lines represent the charm quark propagators.

IV. NUMERICAL ANALYSIS

We use the following values of the quark masses and various condensates in the QCD sum rule analysis [14, 29, 34, 35]. The charm and bottom quark masses are the running masses in the \overline{MS} scheme:

$$\begin{aligned}
m_c(m_c) &= (1.23 \pm 0.09) \text{ GeV}, \\
m_b(m_b) &= (4.20 \pm 0.07) \text{ GeV}, \\
\langle \bar{q}q \rangle &= -(0.23 \pm 0.03)^3 \text{ GeV}^3, \\
\langle \bar{q}g_s \sigma \cdot Gq \rangle &= -M_0^2 \langle \bar{q}q \rangle, \\
M_0^2 &= (0.8 \pm 0.2) \text{ GeV}^2, \\
\langle \bar{s}s \rangle / \langle \bar{q}q \rangle &= 0.8 \pm 0.2, \\
\langle g_s^2 GG \rangle &= 0.88 \text{ GeV}^4, \\
\langle g_s^3 fGGG \rangle &= 0.045 \text{ GeV}^6.
\end{aligned} \tag{11}$$

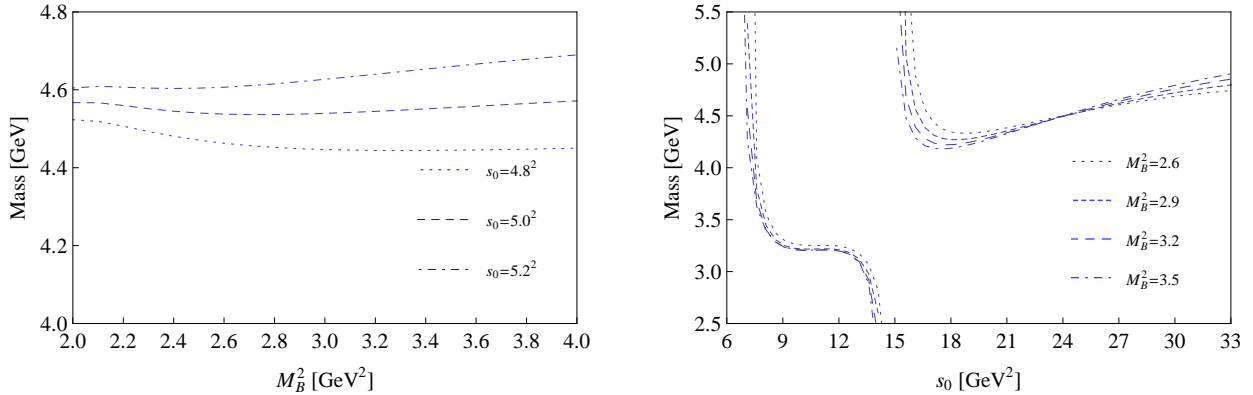


FIG. 2: The variation of M_X with M_B^2 (Left) and s_0 (Right) for the current η_2 .

The Borel mass M_B and the threshold value s_0 are two pivotal parameters in the numerical analysis. The working region of the Borel parameter is determined by the convergence of the operator product expansion and the pole contribution. The requirement of the convergence of OPE leads to the lower bound M_{min}^2 of the Borel parameter. The upper bound M_{max}^2 of the Borel parameter results from the requirement of the pole contribution.

The four quark condensate $\langle \bar{q}q \rangle^2$ is negative and the most important condensate correction numerically. Its absolute value is much bigger than the gluon condensate $\langle g^2 G^2 \rangle$ and the dimension 8 condensate $\langle \bar{q}g\sigma \cdot Gq \rangle \langle \bar{q}q \rangle$. Technically, we require that the four quark condensate be less than one third of the perturbative term to ensure the convergence of OPE, which results at the lower bound of the Borel working window, $M_{min}^2 \sim 2.4 \text{ GeV}$.

The pole contribution (PC) is defined as

$$\frac{\int_{4m_c^2}^{s_0} ds e^{-s/M_B^2} \rho(s)}{\int_{4m_c^2}^{\infty} ds e^{-s/M_B^2} \rho(s)}, \tag{12}$$

which depends on both the Borel mass M_B and the threshold value s_0 . s_0 is chosen around the region where the variation of m_X with M_B^2 is the minimum. For example, we choose $s_0 \sim 25 \text{ GeV}^2$ from the variation of the mass with s_0 as shown in Figs. 2 and 3. Requiring that the PC is larger than 40%, one gets the upper bound M_{max}^2 of the Borel parameter M_B^2 . We list the working range of the Borel parameter for the ten tetraquark currents $\eta_1 \sim \eta_{10}$ in table I. The masses are extracted using these threshold values and $M_B^2 = 3.5 \text{ GeV}^2$, which are also listed in Table I. Only the errors which arise from the uncertainty of the threshold values and variation of the Borel parameter are taken into account. Other possible error sources include the truncation of the OPE series and the uncertainty of the condensate values etc. The last column is the pole contribution.

	Currents	$s_0(\text{GeV}^2)$	$[M_{\min}^2, M_{\max}^2]$	$m_X(\text{GeV})$	PC(%)
$J^{PC} = 0^{--}$	η_1	25	$2.4 \sim 3.6$	—	-
	η_2	25	$2.4 \sim 3.7$	4.55 ± 0.11	46.3
	η_3	25	$2.4 \sim 3.7$	—	-
	η_4	25	$2.4 \sim 3.7$	4.55 ± 0.11	45.9
$J^{PC} = 0^{-+}$	η_5	25	$2.4 \sim 3.6$	—	-
	η_6	25	$2.4 \sim 4.1$	4.72 ± 0.10	53.8
	η_7	25	$2.4 \sim 3.8$	—	-
	η_8	25	$2.4 \sim 3.7$	—	-
	η_9	25	$2.4 \sim 3.7$	4.55 ± 0.11	45.9
	η_{10}	27	$2.4 \sim 4.2$	4.67 ± 0.10	56.8

TABLE I: The threshold value, Borel window, mass and pole contribution for $\eta_1 \sim \eta_{10}$. The mass and pole contribution are calculated at $M_B^2 = 3.5 \text{ GeV}^2$.

From the variation of the mass with s_0 , there is a plateau in the region of $s_0 = 9 \sim 13 \text{ GeV}^2$ for $\eta_2, \eta_4, \eta_6, \eta_9, \eta_{10}$ as can be seen in Fig. 2. This plateau looks like a resonance signal. However, it's just an unphysical artifact because both the numerator and denominator in Eq.(10) are negative within this region. The variation of M_X with the Borel parameter is weak.

For $\eta_1, \eta_3, \eta_5, \eta_7, \eta_8$, the extracted mass M_X grows monotonically with the threshold value. Also the variation of M_X with the Borel parameter is significant. So we do not present the numerical values in Table I for these currents. These currents may couple to the $0^{--}, 0^{-+}$ states very weakly. The continuum contribution may be quite large. These two factors may lead to the above unstable mass sum rules.

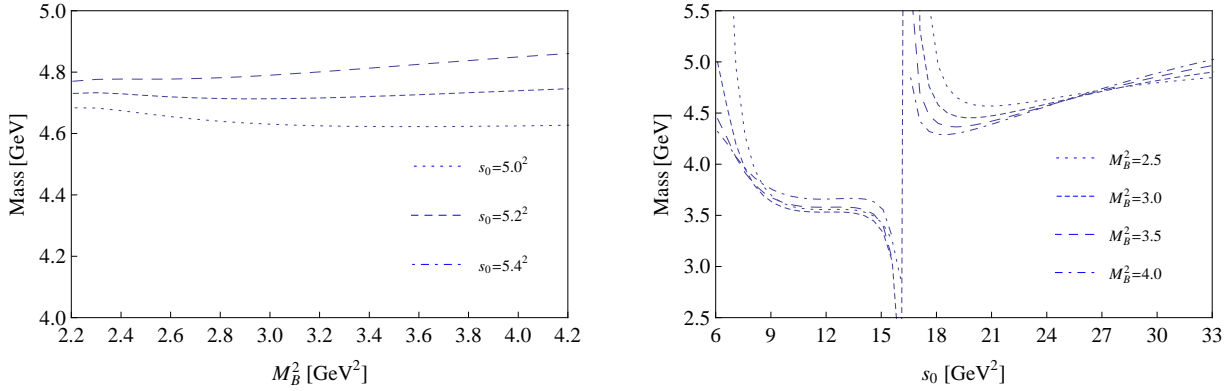


FIG. 3: The variation of M_X with M_B^2 (Left) and s_0 (Right) for the current η_6 .

Replacing m_c with m_b and repeating the same analysis procedures done above, we collect the results of the bottomonium-like systems in Table II.

	Currents	$s_0(\text{GeV}^2)$	$[M_{\min}^2, M_{\max}^2]$	$m_{X_b}(\text{GeV})$	PC(%)
$J^{PC} = 0^{--}$	η_{1b}	11.2^2	$6.4 \sim 9.4$	—	-
	η_{2b}	11.2^2	$6.4 \sim 9.5$	10.64 ± 0.12	45.2
	η_{3b}	11.2^2	$6.4 \sim 9.5$	—	-
	η_{4b}	11.2^2	$6.4 \sim 9.5$	10.64 ± 0.12	45.1
$J^{PC} = 0^{-+}$	η_{5b}	11.2^2	$6.4 \sim 9.4$	—	-
	η_{6b}	11.2^2	$6.4 \sim 9.4$	10.67 ± 0.11	44.2
	η_{7b}	11.2^2	$6.4 \sim 9.7$	—	-
	η_{8b}	11.2^2	$6.4 \sim 9.6$	—	-
	η_{9b}	11.2^2	$6.4 \sim 9.5$	10.64 ± 0.12	45.1
	η_{10b}	11.2^2	$6.4 \sim 9.5$	10.64 ± 0.11	45.6

TABLE II: The threshold value, Borel window, mass and pole contribution for $\eta_{1b} \sim \eta_{10b}$. The mass and pole contribution are calculated at $M_B^2 = 9.0 \text{ GeV}^2$.

V. SUMMARY

We have constructed the charmonium-like tetraquark interpolating currents with $J^{PC} = 0^{--}, 0^{-+}$ using the diquark-antidiquark fields. Then we calculated the correlation functions and the spectral densities of these currents. Both the dimension 3 quark condensate and dimension 5 quark gluon mixed condensate vanish if we take $m_{u,d} = 0$. The special Lorenz structures of the currents prohibit their appearance in the OPE. The four quark condensate $\langle \bar{q}q \rangle^2$ becomes the most important power correction numerically. It is much bigger than the gluon condensates $\langle g^2 GG \rangle$, $\langle g^3 fGGG \rangle$ and the dimension 8 condensate $\langle \bar{q}g\sigma \cdot Gq \rangle \langle \bar{q}q \rangle$.

In the working region of the Borel parameter, the variation of the extracted mass with s_0 and M_B is stable for the currents $\eta_2, \eta_4, \eta_6, \eta_9, \eta_{10}$. For the 0^{--} charmonium-like states, its mass is around 4.5 GeV. For the 0^{-+} charmonium-like state, the mass is around 4.6 GeV. For the 0^{--} and 0^{-+} bottomonium-like states, their masses are around 10.6 GeV. It's interesting to note that the extracted mass value ~ 4.5 GeV of the 0^{--} charmonium-like state is quite close to the mass value $4.1 \sim 4.4$ GeV in Ref. [25].

The possible decay modes of the 0^{--} charmonium-like state are straightforward after making Fierz transformation to the diquark type interpolating currents in Eq. 2. They can be expressed in terms of the linear combination of the meson-meson type of operators such as: $(\bar{q}_a \gamma_\mu q_a)(\bar{c}_b \gamma^\mu \gamma_5 c_b)$, $(\bar{q}_a \gamma_\mu \gamma_5 q_a)(\bar{c}_b \gamma^\mu c_b)$, $(\bar{q}_a \gamma_\mu c_a)(\bar{c}_b \gamma^\mu \gamma_5 q_b) + (\bar{q}_a \gamma_\mu \gamma_5 c_a)(\bar{c}_b \gamma^\mu q_b)$, $(\bar{q}_a c_a)(\bar{c}_b \gamma_5 q_b) - (\bar{q}_a \gamma_5 c_a)(\bar{c}_b q_b)$.

There are two types of the 0^{--} charmonium-like state with different isospin and G-parity: $I^G = 1^+$ and $I^G = 0^-$. Considering the conservation of the isospin, G-parity and C parity, we collect the S-wave and P-wave decay modes of the possible 0^{--} charmonium-like state in Table III.

Clearly the S-wave decay modes are dominant. The S-wave decay products always contain a P-wave and S-wave meson pair. Such a decay pattern is also characteristic of the hybrid meson. Although the exotic 0^{--} state can not be composed of a $c\bar{c}$ pair, it can be a $cG\bar{c}$ hybrid state. In fact, the 0^{--} charmonium-like tetraquark operator and the 0^{--} $cG\bar{c}$ hybrid operator probably couple to the same 0^{--} physical state.

This interesting 0^{--} state may be searched for experimentally at facilities such as Super-B factories, PANDE, LHC and RHIC in the future. Especially at RHIC, plenty of charm, anti-charm and light quarks are produced simultaneously which may be helpful to the formation of the 0^{--} charmonium-like state.

I^G	<i>S</i> -wave	<i>P</i> -wave
0^-	$D^*(2007)^0 D_1(2420)^0 + c.c.$, $D_0^*(2400)^0 \bar{D}^0(1865) + c.c.$, $\omega(782)\chi_{c1}(1P)$, $J/\psi f_1(1285)$	$D^0(1865)D^*(2007)^0 + c.c.$, $D^*(2007)^0 \bar{D}^*(2007)^0$, $J/\psi\eta$, $J/\psi\eta'$, $\psi(2S)\eta$, $\eta_c(1S)\omega$, $\eta_c(2S)\omega$, $h_c(1P)\sigma$, $h_c(1P)f_0(980)$
1^+	$D^*(2007)^0 D_1(2420)^0 + c.c.$, $D_0^*(2400)^0 \bar{D}^0(1865) + c.c.$, $\rho(770)\chi_{c1}(1P)$, $J/\psi a_1(1260)$	$D^0(1865)D^*(2007)^0 + c.c.$, $D^*(2007)^0 \bar{D}^*(2007)^0$, $\eta_c(1S)\rho$, $\eta_c(2S)\rho$, $h_c(1P)a_0(980)$, $J/\psi\pi$, $J/\psi\pi_1(1400)$, $\psi(2S)\pi$

TABLE III: The possible decay modes of the 0^{--} charmonium-like state.

Acknowledgments

The authors thank Professor W. Z. Deng for useful discussions. W. Chen is grateful for J. R. Zhang, M.Q. Huang and M. E. Bracco for their helpful email discussions. This project was supported by the National Natural Science Foundation of China under Grants 10625521, 10721063 and Ministry of Science and Technology of China (2009CB825200).

-
- [1] S. K. Choi et al., Phys. Rev. Lett **91**, 262001 (2003).
[2] S. K. Choi et al., Phys. Rev. Lett **94**, 182002 (2005).
[3] B. Aubert et al., BABAR Collaboration, Phys. Rev. Lett **95**, 142001 (2005).
[4] C. Z. Yuan et al., Belle Collaboration, Phys. Rev. Lett **99**, 182004 (2007).
[5] S. Uehara et al., Phys. Rev. Lett **96**, 082003 (2006).
[6] K. Abe et al., Phys. Rev. Lett **98**, 082001 (2007).
[7] B. Aubert et al., BABAR Collaboration, Phys. Rev. Lett **98**, 212001 (2007).

- [8] X. L. Wang et al., Belle Collaboration, Phys. Rev. Lett **99**, 142002 (2007).
- [9] S. K. Choi et al., Belle Collaboration, Phys. Rev. Lett **100**, 142001 (2008).
- [10] R. Mizuk et al., Belle Collaboration, Phys. Rev. D **78**, 072004 (2008).
- [11] T. Aaltonen et al., CDF Collaboration, Phys. Rev. Lett **102**, 242002 (2009).
- [12] E. S. Swanson, Phys. Rep. **429**, 243 (2006).
- [13] S. L. Zhu, Int. J. Mod. Phys. E **17**, 283 (2008).
- [14] C. Amsler et al., (Particle Data Group), Phys. Lett. B **667**, 1 (2008).
- [15] M. Bracko, arXiv:0907.1358 [hep-ex].
- [16] F. E. Close and S. Godfrey, Phys. Let. B **574**, 210 (2003).
- [17] E. S. Swanson, Phys. Lett. B **598**, 197 (2004); E. S. Swanson, Phys. Lett. B **588**, 189 (2004); L. Maiani, A. D. Polosa, and V. Riquer, Phys. Rev. Lett **99**, 182003 (2007); T. Fernandez-Carames, A. Valcarce, and J. Vijande, Phys. Rev. Lett **103**, 222001 (2009).
- [18] R. D. Matheus, S. Narison, M. Nielsen, and J. M. Richard, Phys. Rev. D **75**, 014005 (2007).
- [19] X. Liu, Y.R. Liu, W. Z Deng, and S. L. Zhu, Phys. Rev. D **77**, 094015 (2008); X. Liu, Y.R. Liu, W. Z Deng, and S. L. Zhu, Phys. Rev. D **77**, 034003 (2008); Su Houng Lee, A. Mihara, F. Navarra, and M. Nielsen, Phys. Lett. B **661**, 28 (2008); C. Meng and K. T. Chao, arXiv:0708.4222[hep-ph]; G. J. Ding, arXiv:0711.1485[hep-ph].
- [20] M. E. Bracco, S. H. Lee, M. Nielsen, and R. Rodrigues da Silva, Phys. Lett. B **671**, 240 (2009); L. Maiani, A. D. Polosa, and V. Riquer, New J. Phys. **10**(2008) 073004.
- [21] F. E. Close and P. R. Page, Phys. Lett. B **628**, 215 (2005).
- [22] L. Maiani, V. Riquer, F. Piccinini, and A. D. Polosa, Phys. Rev. D **72**, 031502 (2005).
- [23] X. Liu and S. L.Zhu, Phys. Rev. D **80**, 017502 (2009); N. Mahajan Phys. Lett. B **679**, 228 (2009); T. Branz, T. Gutsche, and V. E. Lyubovitskij, Phys. Rev. D **80**, 054019 (2009); G. J. Ding, Eur. Phys. J. C **64** 297 (2009).
- [24] Bai-Qing Li and Kuang-Ta Chao, Phys. Rev. D **79**, 094004 (2009).
- [25] Kuang-Ta Chao, Nucl. Phys. B **169**, 281(1980); Nucl. Phys. B**183**, 435(1981).
- [26] Chun-Kun Jiao, Wei Chen, Hua-Xing Chen, and Shi-Lin Zhu, Phys. Rev. D **79**, 114034 (2009).
- [27] H. X. Chen, A. Hosaka, and S. L. Zhu, Phys. Rev. D **78**, 054017 (2008); D78, 117502 (2008).
- [28] H. X. Chen, A. Hosaka, and S. L. Zhu, Phys. Rev. D **74**, 054001 (2006); D76, 094025 (2007); Phys. Lett. B650, 369 (2007); H. X. Chen, X. Liu, A. Hosaka, and S. L. Zhu, Phys. Rev. D78, 034012 (2008).
- [29] M. A. Shifman, A. I. Vainshtein, and V. I. Zakharov, Nucl. Phys. B **147**, 385 (1979).
- [30] L. J. Reinders, H. Rubinstein, and S. Yazaki, Phys. Rept. **127**, 1 (1985).
- [31] P. Colangelo and A. Khodjamirian, Frontier of Particle Physics V.**3***, 1495-1576 (2000).
- [32] R. D. Matheus, F. S. Navarra, M. Nielsen, and C. M. Zanetti, Phys. Rev. D **80**, 056002 (2009).
- [33] J. R. Zhang and M. Q. Huang, Phys. Rev. D **80**, 056004 (2009).
- [34] M. Eidermuller and M. Jamin, Phys. Lett. B **498**, 203 (2001).
- [35] M. Jamin and A. Pich, Nucl. Phys. Proc. Suppl. **74**, 300 (1999).
- [36] S. H. Lee, K. Morita, and M. Nielsen, Nucl. Phys. A **815**, 29 (2009).
- [37] Z. G. Wang, Eur. Phys. J. C **62**, 375 (2009); Phys. Rev. D **79**, 094027 (2009).

Appendix A: THE SPECTRAL DENSITIES

In this appendix we show the spectral densities of the tetraquark interpolating currents defined in Eqs. (2)-(3). The same subscripts are used to denote the results for the currents $\eta_1, \eta_2, \eta_3, \eta_4, \eta_5, \eta_6, \eta_7, \eta_8, \eta_9, \eta_{10}$:

$$\rho^{OPE} = \rho^{pert}(s) + \rho^{\langle\bar{q}q\rangle}(s) + \rho^{\langle G^2 \rangle}(s) + \rho^{mix}(s) + \rho^{\langle\bar{q}q\rangle^2}(s) \quad (\text{A1})$$

For the expressions below, the integration limits are:

$$\begin{aligned} \alpha_{max} &= \frac{1 + \sqrt{1 - 4m_c^2/s}}{2}, & \alpha_{min} &= \frac{1 - \sqrt{1 - 4m_c^2/s}}{2} \\ \beta_{max} &= 1 - \alpha, & \beta_{min} &= \frac{\alpha m_c^2}{\alpha s - m_c^2}. \end{aligned}$$

1. The spectral densities of the interpolating currents with the quantum numbers $J^{PC} = 0^{--}$:

For η_1 :

$$\begin{aligned}
\rho_1^{pert}(s) &= \frac{1}{2^7 \pi^6} \int_{\alpha_{min}}^{\alpha_{max}} \frac{d\alpha}{\alpha^3} \int_{\beta_{min}}^{\beta_{max}} \frac{(1-\alpha-\beta)^2}{\beta^3} [(\alpha+\beta)m_c^2 - 3\alpha\beta s][(\alpha+\beta)m_c^2 - \alpha\beta s]^3, \\
\rho_1^{\langle\bar{q}q\rangle}(s) &= 0, \\
\rho_1^{\langle GG \rangle}(s) &= \frac{\langle g_s^2 GG \rangle}{2^7 \pi^6} \int_{\alpha_{min}}^{\alpha_{max}} \frac{d\alpha}{\alpha^2} \int_{\beta_{min}}^{\beta_{max}} \left\{ \frac{(1-\alpha-\beta)^2 m_c^2}{3\alpha} [2(\alpha+\beta)m_c^2 - 3\alpha\beta s] \right. \\
&\quad \left. - \frac{1-\alpha-\beta}{2\beta} [(\alpha+\beta)m_c^2 - 2\alpha\beta s][(\alpha+\beta)m_c^2 - \alpha\beta s] \right\}, \\
\rho_1^{mix}(s) &= 0, \\
\rho_1^{\langle\bar{q}q\rangle^2}(s) &= -\frac{m_c^2 \langle\bar{q}q\rangle^2}{3\pi^2} \sqrt{1-4m_c^2/s}, \tag{A2}
\end{aligned}$$

$$\begin{aligned}
\Pi_1^{mix\langle\bar{q}q\rangle}(M_B^2) &= -\frac{m_c^2 \langle\bar{q}g_s\sigma \cdot Gq\rangle \langle\bar{q}q\rangle}{12\pi^2} \int_0^1 \frac{d\alpha}{\alpha} \left(\frac{2m_c^2}{\alpha M_B^2} + 1 \right) e^{-\frac{m_c^2}{\alpha(1-\alpha)M_B^2}}, \\
\Pi_1^{\langle GGG \rangle}(M_B^2) &= -\frac{\langle g_s^3 f GGG \rangle}{3 \times 2^8 \pi^6} \int_0^1 d\alpha \int_0^{\beta_{max}} d\beta \\
&\quad \left\{ \frac{\ln(\alpha\beta(1-\alpha-\beta)M_B^4) - 2\ln 2 - \gamma_E}{\alpha\beta} [12(\alpha\beta M_B^2)^2 + 6\alpha\beta M_B^2(\alpha+\beta)m_c^2 + (\alpha+\beta)^2 m_c^4] \right. \\
&\quad + \frac{33(\alpha\beta M_B^2)^2 + 12\alpha\beta M_B^2(\alpha+\beta)m_c^2 + (\alpha+\beta)^2 m_c^4}{\alpha\beta} + \frac{(1-\alpha-\beta)^2 m_c^2}{\alpha^4} [2\alpha\beta M_B^2 + (\alpha+\beta)m_c^2] \\
&\quad \left. - \frac{(1-\alpha-\beta)^2}{2\alpha^3} [3\alpha\beta M_B^4 + M_B^2(\alpha+\beta)m_c^2] \right\} e^{-\frac{(\alpha+\beta)m_c^2}{\alpha\beta M_B^2}}.
\end{aligned}$$

For η_2 :

$$\begin{aligned}
\rho_2^{pert}(s) &= \frac{1}{2^5 \pi^6} \int_{\alpha_{min}}^{\alpha_{max}} \frac{d\alpha}{\alpha^3} \int_{\beta_{min}}^{\beta_{max}} \frac{(1-\alpha-\beta)^2}{\beta^3} [(\alpha+\beta)m_c^2 - 3\alpha\beta s][(\alpha+\beta)m_c^2 - \alpha\beta s]^3, \\
\rho_2^{\langle\bar{q}q\rangle}(s) &= 0, \\
\rho_2^{\langle GG \rangle}(s) &= \frac{\langle g_s^2 GG \rangle}{2^5 \pi^6} \int_{\alpha_{min}}^{\alpha_{max}} \frac{d\alpha}{\alpha^2} \int_{\beta_{min}}^{\beta_{max}} \left\{ \frac{(1-\alpha-\beta)^2 m_c^2}{3\alpha} [2(\alpha+\beta)m_c^2 - 3\alpha\beta s] \right. \\
&\quad \left. + \frac{5(1-\alpha-\beta)}{4\beta} [(\alpha+\beta)m_c^2 - 2\alpha\beta s][(\alpha+\beta)m_c^2 - \alpha\beta s] \right\}, \\
\rho_2^{mix}(s) &= 0, \\
\rho_2^{\langle\bar{q}q\rangle^2}(s) &= -\frac{4m_c^2 \langle\bar{q}q\rangle^2}{3\pi^2} \sqrt{1-4m_c^2/s}, \tag{A3}
\end{aligned}$$

$$\begin{aligned}
\Pi_2^{mix\langle\bar{q}q\rangle}(M_B^2) &= -\frac{m_c^2 \langle\bar{q}g_s\sigma \cdot Gq\rangle \langle\bar{q}q\rangle}{6\pi^2} \int_0^1 \frac{d\alpha}{\alpha} \left(\frac{4m_c^2}{\alpha M_B^2} - 5 \right) e^{-\frac{m_c^2}{\alpha(1-\alpha)M_B^2}}, \\
\Pi_2^{\langle GGG \rangle}(M_B^2) &= -\frac{\langle g_s^3 f GGG \rangle}{3 \times 2^6 \pi^6} \int_0^1 d\alpha \int_0^{\beta_{max}} d\beta \\
&\quad \left\{ \frac{\ln(\alpha\beta(1-\alpha-\beta)M_B^4) - 2\ln 2 - \gamma_E}{\alpha\beta} [12(\alpha\beta M_B^2)^2 + 6\alpha\beta M_B^2(\alpha+\beta)m_c^2 + (\alpha+\beta)^2 m_c^4] \right. \\
&\quad + \frac{33(\alpha\beta M_B^2)^2 + 12\alpha\beta M_B^2(\alpha+\beta)m_c^2 + (\alpha+\beta)^2 m_c^4}{\alpha\beta} + \frac{(1-\alpha-\beta)^2 m_c^2}{\alpha^4} [2\alpha\beta M_B^2 + (\alpha+\beta)m_c^2] \\
&\quad \left. - \frac{(1-\alpha-\beta)^2}{2\alpha^3} [3\alpha\beta M_B^4 + M_B^2(\alpha+\beta)m_c^2] \right\} e^{-\frac{(\alpha+\beta)m_c^2}{\alpha\beta M_B^2}}.
\end{aligned}$$

For η_3 :

$$\begin{aligned}
\rho_3^{pert}(s) &= \frac{1}{2^6\pi^6} \int_{\alpha_{min}}^{\alpha_{max}} \frac{d\alpha}{\alpha^3} \int_{\beta_{min}}^{\beta_{max}} \frac{(1-\alpha-\beta)^2}{\beta^3} [(\alpha+\beta)m_c^2 - 3\alpha\beta s][(\alpha+\beta)m_c^2 - \alpha\beta s]^3, \\
\rho_3^{\langle\bar{q}q\rangle}(s) &= 0, \\
\rho_3^{\langle GG \rangle}(s) &= \frac{\langle g_s^2 GG \rangle}{2^6\pi^6} \int_{\alpha_{min}}^{\alpha_{max}} \frac{d\alpha}{\alpha^2} \int_{\beta_{min}}^{\beta_{max}} \left\{ \frac{(1-\alpha-\beta)^2 m_c^2}{3\alpha} [2(\alpha+\beta)m_c^2 - 3\alpha\beta s] \right. \\
&\quad \left. + \frac{1-\alpha-\beta}{2\beta} [(\alpha+\beta)m_c^2 - 2\alpha\beta s][(\alpha+\beta)m_c^2 - \alpha\beta s] \right\}, \\
\rho_3^{mix}(s) &= 0, \\
\rho_3^{\langle\bar{q}q\rangle^2}(s) &= -\frac{2m_c^2 \langle\bar{q}q\rangle^2}{3\pi^2} \sqrt{1-4m_c^2/s},
\end{aligned} \tag{A4}$$

$$\begin{aligned}
\Pi_3^{mix\langle\bar{q}q\rangle}(M_B^2) &= -\frac{m_c^2 \langle\bar{q}g_s\sigma \cdot Gq\rangle \langle\bar{q}q\rangle}{6\pi^2} \int_0^1 \frac{d\alpha}{\alpha} \left(\frac{2m_c^2}{\alpha M_B^2} - 1 \right) e^{-\frac{m_c^2}{\alpha(1-\alpha)M_B^2}}, \\
\Pi_3^{\langle GGG \rangle}(M_B^2) &= -\frac{\langle g_s^3 f GGG \rangle}{3 \times 2^6\pi^6} \int_0^1 d\alpha \int_0^{\beta_{max}} d\beta \\
&\quad \left\{ \frac{\ln(\alpha\beta(1-\alpha-\beta)M_B^4) - 2\ln 2 - \gamma_E}{\alpha\beta} [12(\alpha\beta M_B^2)^2 + 6\alpha\beta M_B^2(\alpha+\beta)m_c^2 + (\alpha+\beta)^2 m_c^4] \right. \\
&\quad + \frac{33(\alpha\beta M_B^2)^2 + 12\alpha\beta M_B^2(\alpha+\beta)m_c^2 + (\alpha+\beta)^2 m_c^4}{\alpha\beta} + \frac{(1-\alpha-\beta)^2 m_c^2}{\alpha^4} [2\alpha\beta M_B^2 + (\alpha+\beta)m_c^2] \\
&\quad \left. - \frac{(1-\alpha-\beta)^2}{2\alpha^3} [3\alpha\beta M_B^4 + M_B^2(\alpha+\beta)m_c^2] \right\} e^{-\frac{(\alpha+\beta)m_c^2}{\alpha\beta M_B^2}}.
\end{aligned}$$

For η_4 :

$$\begin{aligned}
\rho_4^{pert}(s) &= \frac{1}{2^8\pi^6} \int_{\alpha_{min}}^{\alpha_{max}} \frac{d\alpha}{\alpha^3} \int_{\beta_{min}}^{\beta_{max}} \frac{(1-\alpha-\beta)^2}{\beta^3} [(\alpha+\beta)m_c^2 - 3\alpha\beta s][(\alpha+\beta)m_c^2 - \alpha\beta s]^3, \\
\rho_4^{\langle\bar{q}q\rangle}(s) &= 0, \\
\rho_4^{\langle GG \rangle}(s) &= \frac{\langle g_s^2 GG \rangle}{2^8\pi^6} \int_{\alpha_{min}}^{\alpha_{max}} \frac{d\alpha}{\alpha^2} \int_{\beta_{min}}^{\beta_{max}} \left\{ \frac{(1-\alpha-\beta)^2 m_c^2}{3\alpha} [2(\alpha+\beta)m_c^2 - 3\alpha\beta s] \right. \\
&\quad \left. + \frac{1-\alpha-\beta}{\beta} [(\alpha+\beta)m_c^2 - 2\alpha\beta s][(\alpha+\beta)m_c^2 - \alpha\beta s] \right\}, \\
\rho_4^{mix}(s) &= 0, \\
\rho_4^{\langle\bar{q}q\rangle^2}(s) &= -\frac{m_c^2 \langle\bar{q}q\rangle^2}{6\pi^2} \sqrt{1-4m_c^2/s},
\end{aligned} \tag{A5}$$

$$\begin{aligned}
\Pi_4^{mix\langle\bar{q}q\rangle}(M_B^2) &= -\frac{m_c^2 \langle\bar{q}g_s\sigma \cdot Gq\rangle \langle\bar{q}q\rangle}{12\pi^2} \int_0^1 \frac{d\alpha}{\alpha} \left(\frac{m_c^2}{\alpha M_B^2} - 1 \right) e^{-\frac{m_c^2}{\alpha(1-\alpha)M_B^2}}, \\
\Pi_4^{\langle GGG \rangle}(M_B^2) &= -\frac{\langle g_s^3 f GGG \rangle}{3 \times 2^9\pi^6} \int_0^1 d\alpha \int_0^{\beta_{max}} d\beta \\
&\quad \left\{ \frac{\ln(\alpha\beta(1-\alpha-\beta)M_B^4) - 2\ln 2 - \gamma_E}{\alpha\beta} [12(\alpha\beta M_B^2)^2 + 6\alpha\beta M_B^2(\alpha+\beta)m_c^2 + (\alpha+\beta)^2 m_c^4] \right. \\
&\quad + \frac{33(\alpha\beta M_B^2)^2 + 12\alpha\beta M_B^2(\alpha+\beta)m_c^2 + (\alpha+\beta)^2 m_c^4}{\alpha\beta} + \frac{(1-\alpha-\beta)^2 m_c^2}{\alpha^4} [2\alpha\beta M_B^2 + (\alpha+\beta)m_c^2] \\
&\quad \left. - \frac{(1-\alpha-\beta)^2}{2\alpha^3} [3\alpha\beta M_B^4 + M_B^2(\alpha+\beta)m_c^2] \right\} e^{-\frac{(\alpha+\beta)m_c^2}{\alpha\beta M_B^2}}.
\end{aligned}$$

2. The spectral densities of the interpolating currents with the quantum numbers $J^{PC} = 0^{-+}$:

For η_5 :

$$\begin{aligned}
\rho_5^{pert}(s) &= \frac{1}{2^7 \pi^6} \int_{\alpha_{min}}^{\alpha_{max}} \frac{d\alpha}{\alpha^3} \int_{\beta_{min}}^{\beta_{max}} \frac{(1-\alpha-\beta)^2}{\beta^3} [(\alpha+\beta)m_c^2 - 3\alpha\beta s][(\alpha+\beta)m_c^2 - \alpha\beta s]^3, \\
\rho_5^{\langle\bar{q}q\rangle}(s) &= 0, \\
\rho_5^{\langle GG \rangle}(s) &= \frac{\langle g_s^2 GG \rangle}{2^7 \pi^6} \int_{\alpha_{min}}^{\alpha_{max}} \frac{d\alpha}{\alpha^2} \int_{\beta_{min}}^{\beta_{max}} \left\{ \frac{(1-\alpha-\beta)^2 m_c^2}{3\alpha} [2(\alpha+\beta)m_c^2 - 3\alpha\beta s] \right. \\
&\quad \left. - \frac{1-\alpha-\beta}{2\beta} [(\alpha+\beta)m_c^2 - 2\alpha\beta s][(\alpha+\beta)m_c^2 - \alpha\beta s] \right\}, \\
\rho_5^{mix}(s) &= 0, \\
\rho_5^{\langle\bar{q}q\rangle^2}(s) &= -\frac{m_c^2 \langle\bar{q}q\rangle^2}{3\pi^2} \sqrt{1-4m_c^2/s},
\end{aligned} \tag{A6}$$

$$\begin{aligned}
\Pi_5^{mix\langle\bar{q}q\rangle}(M_B^2) &= -\frac{m_c^2 \langle\bar{q}g_s\sigma \cdot Gq\rangle \langle\bar{q}q\rangle}{12\pi^2} \int_0^1 \frac{d\alpha}{\alpha} \left(\frac{2m_c^2}{\alpha M_B^2} + 1 \right) e^{-\frac{m_c^2}{\alpha(1-\alpha)M_B^2}}, \\
\Pi_5^{\langle GGG \rangle}(M_B^2) &= -\frac{\langle g_s^3 f GGG \rangle}{3 \times 2^8 \pi^6} \int_0^1 d\alpha \int_0^{\beta_{max}} d\beta \\
&\quad \left\{ \frac{\ln(\alpha\beta(1-\alpha-\beta)M_B^4) - 2\ln 2 - \gamma_E}{\alpha\beta} [12(\alpha\beta M_B^2)^2 + 6\alpha\beta M_B^2(\alpha+\beta)m_c^2 + (\alpha+\beta)^2 m_c^4] \right. \\
&\quad + \frac{33(\alpha\beta M_B^2)^2 + 12\alpha\beta M_B^2(\alpha+\beta)m_c^2 + (\alpha+\beta)^2 m_c^4}{\alpha\beta} + \frac{(1-\alpha-\beta)^2 m_c^2}{\alpha^4} [2\alpha\beta M_B^2 + (\alpha+\beta)m_c^2] \\
&\quad \left. - \frac{(1-\alpha-\beta)^2}{2\alpha^3} [3\alpha\beta M_B^4 + M_B^2(\alpha+\beta)m_c^2] \right\} e^{-\frac{(\alpha+\beta)m_c^2}{\alpha\beta M_B^2}}.
\end{aligned}$$

For η_6 :

$$\begin{aligned}
\rho_6^{pert}(s) &= \frac{3}{2^6 \pi^6} \int_{\alpha_{min}}^{\alpha_{max}} \frac{d\alpha}{\alpha^3} \int_{\beta_{min}}^{\beta_{max}} \frac{(1-\alpha-\beta)^2}{\beta^3} [(\alpha+\beta)m_c^2 - 3\alpha\beta s][(\alpha+\beta)m_c^2 - \alpha\beta s]^3, \\
\rho_6^{\langle\bar{q}q\rangle}(s) &= 0, \\
\rho_6^{\langle GG \rangle}(s) &= \frac{\langle g_s^2 GG \rangle}{2^6 \pi^6} \int_{\alpha_{min}}^{\alpha_{max}} \frac{d\alpha}{\alpha^2} \int_{\beta_{min}}^{\beta_{max}} \left\{ \frac{(1-\alpha-\beta)^2 m_c^2}{\alpha} [2(\alpha+\beta)m_c^2 - 3\alpha\beta s] \right. \\
&\quad \left. + \frac{(1-\alpha-\beta)^2 + 2\alpha\beta}{4\beta^2} [(\alpha+\beta)m_c^2 - 2\alpha\beta s][(\alpha+\beta)m_c^2 - \alpha\beta s] \right\}, \\
\rho_6^{mix}(s) &= 0, \\
\rho_6^{\langle\bar{q}q\rangle^2}(s) &= -\frac{2m_c^2 \langle\bar{q}q\rangle^2}{\pi^2} \sqrt{1-4m_c^2/s},
\end{aligned} \tag{A7}$$

$$\begin{aligned}
\Pi_6^{mix\langle\bar{q}q\rangle}(M_B^2) &= -\frac{m_c^2 \langle\bar{q}g_s\sigma \cdot Gq\rangle \langle\bar{q}q\rangle}{\pi^2} \int_0^1 \frac{d\alpha}{\alpha^2} \frac{m_c^2}{M_B^2} e^{-\frac{m_c^2}{\alpha(1-\alpha)M_B^2}}, \\
\Pi_6^{\langle GGG \rangle}(M_B^2) &= -\frac{\langle g_s^3 f GGG \rangle}{3 \times 2^7 \pi^6} \int_0^1 d\alpha \int_0^{\beta_{max}} d\beta \\
&\quad \left\{ \frac{\ln(\alpha\beta(1-\alpha-\beta)M_B^4) - 2\ln 2 - \gamma_E}{\alpha\beta} [12(\alpha\beta M_B^2)^2 + 6\alpha\beta M_B^2(\alpha+\beta)m_c^2 + (\alpha+\beta)^2 m_c^4] \right. \\
&\quad + \frac{33(\alpha\beta M_B^2)^2 + 12\alpha\beta M_B^2(\alpha+\beta)m_c^2 + (\alpha+\beta)^2 m_c^4}{\alpha\beta} + \frac{3(1-\alpha-\beta)^2 m_c^2}{\alpha^4} [2\alpha\beta M_B^2 + (\alpha+\beta)m_c^2] \\
&\quad \left. - \frac{3(1-\alpha-\beta)^2}{2\alpha^3} [3\alpha\beta M_B^4 + M_B^2(\alpha+\beta)m_c^2] + \frac{2}{1-\alpha-\beta} [3\alpha\beta M_B^4 + M_B^2(\alpha+\beta)m_c^2] \right\} e^{-\frac{(\alpha+\beta)m_c^2}{\alpha\beta M_B^2}}.
\end{aligned}$$

For η_7 :

$$\begin{aligned}
\rho_7^{pert}(s) &= \frac{1}{2^5 \pi^6} \int_{\alpha_{min}}^{\alpha_{max}} \frac{d\alpha}{\alpha^3} \int_{\beta_{min}}^{\beta_{max}} \frac{(1-\alpha-\beta)^2}{\beta^3} [(\alpha+\beta)m_c^2 - 3\alpha\beta s][(\alpha+\beta)m_c^2 - \alpha\beta s]^3, \\
\rho_7^{\langle\bar{q}q\rangle}(s) &= 0, \\
\rho_7^{\langle GG \rangle}(s) &= \frac{\langle g_s^2 GG \rangle}{3 \times 2^5 \pi^6} \int_{\alpha_{min}}^{\alpha_{max}} \frac{d\alpha}{\alpha^2} \int_{\beta_{min}}^{\beta_{max}} \left\{ \frac{(1-\alpha-\beta)^2 m_c^2}{\alpha} [2(\alpha+\beta)m_c^2 - 3\alpha\beta s] \right. \\
&\quad \left. + \frac{15(1-\alpha-\beta)^2 + 30\alpha\beta}{16\beta^2} [(\alpha+\beta)m_c^2 - 2\alpha\beta s][(\alpha+\beta)m_c^2 - \alpha\beta s] \right\}, \\
\rho_7^{mix}(s) &= 0, \\
\rho_7^{\langle\bar{q}q\rangle^2}(s) &= -\frac{4m_c^2 \langle\bar{q}q\rangle^2}{3\pi^2} \sqrt{1 - 4m_c^2/s},
\end{aligned} \tag{A8}$$

$$\begin{aligned}
\Pi_7^{mix\langle\bar{q}q\rangle}(M_B^2) &= -\frac{2m_c^2 \langle\bar{q}g_s\sigma \cdot Gq\rangle \langle\bar{q}q\rangle}{3\pi^2} \int_0^1 \frac{d\alpha}{\alpha^2} \frac{m_c^2}{M_B^2} e^{-\frac{m_c^2}{\alpha(1-\alpha)M_B^2}}, \\
\Pi_7^{\langle GG \rangle}(M_B^2) &= -\frac{\langle g_s^3 f GGG \rangle}{3 \times 2^6 \pi^6} \int_0^1 d\alpha \int_0^{\beta_{max}} d\beta \\
&\quad \left\{ \frac{\ln(\alpha\beta(1-\alpha-\beta)M_B^4) - 2\ln 2 - \gamma_E}{\alpha\beta} [12(\alpha\beta M_B^2)^2 + 6\alpha\beta M_B^2(\alpha+\beta)m_c^2 + (\alpha+\beta)^2 m_c^4] \right. \\
&\quad + \frac{33(\alpha\beta M_B^2)^2 + 12\alpha\beta M_B^2(\alpha+\beta)m_c^2 + (\alpha+\beta)^2 m_c^4}{\alpha\beta} + \frac{(1-\alpha-\beta)^2 m_c^2}{\alpha^4} [2\alpha\beta M_B^2 + (\alpha+\beta)m_c^2] \\
&\quad \left. - \frac{(1-\alpha-\beta)^2}{2\alpha^3} [3\alpha\beta M_B^4 + M_B^2(\alpha+\beta)m_c^2] \right\} e^{-\frac{(\alpha+\beta)m_c^2}{\alpha\beta M_B^2}}.
\end{aligned}$$

For η_8 :

$$\begin{aligned}
\rho_8^{pert}(s) &= \frac{1}{2^6 \pi^6} \int_{\alpha_{min}}^{\alpha_{max}} \frac{d\alpha}{\alpha^3} \int_{\beta_{min}}^{\beta_{max}} \frac{(1-\alpha-\beta)^2}{\beta^3} [(\alpha+\beta)m_c^2 - 3\alpha\beta s][(\alpha+\beta)m_c^2 - \alpha\beta s]^3, \\
\rho_8^{\langle\bar{q}q\rangle}(s) &= 0, \\
\rho_8^{\langle GG \rangle}(s) &= \frac{\langle g_s^2 GG \rangle}{3 \times 2^6 \pi^6} \int_{\alpha_{min}}^{\alpha_{max}} \frac{d\alpha}{\alpha^2} \int_{\beta_{min}}^{\beta_{max}} \left\{ \frac{(1-\alpha-\beta)^2 m_c^2}{\alpha} [2(\alpha+\beta)m_c^2 - 3\alpha\beta s] \right. \\
&\quad \left. + \frac{3(1-\alpha-\beta)^2 + 6\alpha\beta}{8\beta^2} [(\alpha+\beta)m_c^2 - 2\alpha\beta s][(\alpha+\beta)m_c^2 - \alpha\beta s] \right\}, \\
\rho_8^{mix}(s) &= 0, \\
\rho_8^{\langle\bar{q}q\rangle^2}(s) &= -\frac{2m_c^2 \langle\bar{q}q\rangle^2}{3\pi^2} \sqrt{1 - 4m_c^2/s},
\end{aligned} \tag{A9}$$

$$\begin{aligned}
\Pi_8^{mix\langle\bar{q}q\rangle}(M_B^2) &= -\frac{m_c^2 \langle\bar{q}g_s\sigma \cdot Gq\rangle \langle\bar{q}q\rangle}{3\pi^2} \int_0^1 \frac{d\alpha}{\alpha^2} \frac{m_c^2}{M_B^2} e^{-\frac{m_c^2}{\alpha(1-\alpha)M_B^2}}, \\
\Pi_8^{\langle GG \rangle}(M_B^2) &= -\frac{\langle g_s^3 f GGG \rangle}{3 \times 2^7 \pi^6} \int_0^1 d\alpha \int_0^{\beta_{max}} d\beta \\
&\quad \left\{ \frac{\ln(\alpha\beta(1-\alpha-\beta)M_B^4) - 2\ln 2 - \gamma_E}{\alpha\beta} [12(\alpha\beta M_B^2)^2 + 6\alpha\beta M_B^2(\alpha+\beta)m_c^2 + (\alpha+\beta)^2 m_c^4] \right. \\
&\quad + \frac{33(\alpha\beta M_B^2)^2 + 12\alpha\beta M_B^2(\alpha+\beta)m_c^2 + (\alpha+\beta)^2 m_c^4}{\alpha\beta} + \frac{(1-\alpha-\beta)^2 m_c^2}{\alpha^4} [2\alpha\beta M_B^2 + (\alpha+\beta)m_c^2] \\
&\quad \left. - \frac{(1-\alpha-\beta)^2}{2\alpha^3} [3\alpha\beta M_B^4 + M_B^2(\alpha+\beta)m_c^2] \right\} e^{-\frac{(\alpha+\beta)m_c^2}{\alpha\beta M_B^2}}.
\end{aligned}$$

For η_9 :

$$\begin{aligned}
\rho_9^{pert}(s) &= \frac{1}{2^8 \pi^6} \int_{\alpha_{min}}^{\alpha_{max}} \frac{d\alpha}{\alpha^3} \int_{\beta_{min}}^{\beta_{max}} \frac{(1-\alpha-\beta)^2}{\beta^3} [(\alpha+\beta)m_c^2 - 3\alpha\beta s][(\alpha+\beta)m_c^2 - \alpha\beta s]^3, \\
\rho_9^{\langle\bar{q}q\rangle}(s) &= 0, \\
\rho_9^{\langle GG \rangle}(s) &= \frac{\langle g_s^2 GG \rangle}{2^8 \pi^6} \int_{\alpha_{min}}^{\alpha_{max}} \frac{d\alpha}{\alpha^2} \int_{\beta_{min}}^{\beta_{max}} \left\{ \frac{(1-\alpha-\beta)^2 m_c^2}{3\alpha} [2(\alpha+\beta)m_c^2 - 3\alpha\beta s] \right. \\
&\quad \left. + \frac{1-\alpha-\beta}{\beta} [(\alpha+\beta)m_c^2 - 2\alpha\beta s][(\alpha+\beta)m_c^2 - \alpha\beta s] \right\}, \\
\rho_9^{mix}(s) &= 0, \\
\rho_9^{\langle\bar{q}q\rangle^2}(s) &= -\frac{m_c^2 \langle\bar{q}q\rangle^2}{6\pi^2} \sqrt{1-4m_c^2/s},
\end{aligned} \tag{A10}$$

$$\begin{aligned}
\Pi_9^{mix\langle\bar{q}q\rangle}(M_B^2) &= -\frac{m_c^2 \langle\bar{q}g_s\sigma \cdot Gq\rangle \langle\bar{q}q\rangle}{12\pi^2} \int_0^1 \frac{d\alpha}{\alpha} \left(\frac{m_c^2}{\alpha M_B^2} - 1 \right) e^{-\frac{m_c^2}{\alpha(1-\alpha)M_B^2}}, \\
\Pi_9^{\langle GGG \rangle}(M_B^2) &= -\frac{\langle g_s^3 f GGG \rangle}{3 \times 2^9 \pi^6} \int_0^1 d\alpha \int_0^{\beta_{max}} d\beta \\
&\quad \left\{ \frac{\ln(\alpha\beta(1-\alpha-\beta)M_B^4) - 2\ln 2 - \gamma_E}{\alpha\beta} [12(\alpha\beta M_B^2)^2 + 6\alpha\beta M_B^2(\alpha+\beta)m_c^2 + (\alpha+\beta)^2 m_c^4] \right. \\
&\quad + \frac{33(\alpha\beta M_B^2)^2 + 12\alpha\beta M_B^2(\alpha+\beta)m_c^2 + (\alpha+\beta)^2 m_c^4}{\alpha\beta} + \frac{(1-\alpha-\beta)^2 m_c^2}{\alpha^4} [2\alpha\beta M_B^2 + (\alpha+\beta)m_c^2] \\
&\quad \left. - \frac{(1-\alpha-\beta)^2}{2\alpha^3} [3\alpha\beta M_B^4 + M_B^2(\alpha+\beta)m_c^2] \right\} e^{-\frac{(\alpha+\beta)m_c^2}{\alpha\beta M_B^2}}.
\end{aligned}$$

For η_{10} :

$$\begin{aligned}
\rho_{10}^{pert}(s) &= \frac{3}{2^5 \pi^6} \int_{\alpha_{min}}^{\alpha_{max}} \frac{d\alpha}{\alpha^3} \int_{\beta_{min}}^{\beta_{max}} \frac{(1-\alpha-\beta)^2}{\beta^3} [(\alpha+\beta)m_c^2 - 3\alpha\beta s][(\alpha+\beta)m_c^2 - \alpha\beta s]^3, \\
\rho_{10}^{\langle\bar{q}q\rangle}(s) &= 0, \\
\rho_{10}^{\langle GG \rangle}(s) &= \frac{\langle g_s^2 GG \rangle}{2^6 \pi^6} \int_{\alpha_{min}}^{\alpha_{max}} \frac{d\alpha}{\alpha^2} \int_{\beta_{min}}^{\beta_{max}} \left\{ \frac{2(1-\alpha-\beta)^2 m_c^2}{\alpha} [2(\alpha+\beta)m_c^2 - 3\alpha\beta s] \right. \\
&\quad + \frac{5(1-\alpha-\beta)^2 + 10\alpha\beta}{4\beta^2} [(\alpha+\beta)m_c^2 - 2\alpha\beta s][(\alpha+\beta)m_c^2 - \alpha\beta s] \\
&\quad \left. + \frac{6(1-\alpha-\beta)}{\beta} [(\alpha+\beta)m_c^2 - 2\alpha\beta s][(\alpha+\beta)m_c^2 - \alpha\beta s] \right\}, \\
\rho_{10}^{mix}(s) &= 0, \\
\rho_{10}^{\langle\bar{q}q\rangle^2}(s) &= -\frac{4m_c^2 \langle\bar{q}q\rangle^2}{\pi^2} \sqrt{1-4m_c^2/s},
\end{aligned} \tag{A11}$$

$$\begin{aligned}
\Pi_{10}^{mix\langle\bar{q}q\rangle}(M_B^2) &= -\frac{2m_c^2 \langle\bar{q}g_s\sigma \cdot Gq\rangle \langle\bar{q}q\rangle}{\pi^2} \int_0^1 \frac{d\alpha}{\alpha} \left(\frac{m_c^2}{\alpha M_B^2} - 1 \right) e^{-\frac{m_c^2}{\alpha(1-\alpha)M_B^2}}, \\
\Pi_{10}^{\langle GGG \rangle}(M_B^2) &= -\frac{\langle g_s^3 f GGG \rangle}{3 \times 2^6 \pi^6} \int_0^1 d\alpha \int_0^{\beta_{max}} d\beta \\
&\quad \left\{ \frac{\ln(\alpha\beta(1-\alpha-\beta)M_B^4) - 2\ln 2 - \gamma_E}{\alpha\beta} [12(\alpha\beta M_B^2)^2 + 6\alpha\beta M_B^2(\alpha+\beta)m_c^2 + (\alpha+\beta)^2 m_c^4] \right. \\
&\quad + \frac{33(\alpha\beta M_B^2)^2 + 12\alpha\beta M_B^2(\alpha+\beta)m_c^2 + (\alpha+\beta)^2 m_c^4}{\alpha\beta} + \frac{3(1-\alpha-\beta)^2 m_c^2}{\alpha^4} [2\alpha\beta M_B^2 + (\alpha+\beta)m_c^2] \\
&\quad \left. - \frac{3(1-\alpha-\beta)^2}{2\alpha^3} [3\alpha\beta M_B^4 + M_B^2(\alpha+\beta)m_c^2] + \frac{2}{1-\alpha-\beta} [3\alpha\beta M_B^4 + M_B^2(\alpha+\beta)m_c^2] \right\} e^{-\frac{(\alpha+\beta)m_c^2}{\alpha\beta M_B^2}}.
\end{aligned}$$